Hindawi Publishing Corporation
Journal of Nanomaterials
Volume 2016, Article ID 7089530, 9 pages
http://dx.doi.org/10.1155/2016/7089530

Research Article

Investigation on Nanocomposite Membrane of Multiwalled Carbon Nanotube Reinforced Polycarbonate Blend for Gas Separation

Ayesha Kausar

Nanoscience and Technology Department, National Centre for Physics, Quaid-i-Azam University Campus, Islamabad, Pakistan

Correspondence should be addressed to Ayesha Kausar; asheesgreat@yahoo.com

Received 7 September 2016; Accepted 9 November 2016

Academic Editor: Bhanu P. Singh

Copyright © 2016 Ayesha Kausar. This is an open access article distributed under the Creative Commons Attribution License, which permits unrestricted use, distribution, and reproduction in any medium, provided the original work is properly cited.

Carbon nanotube has been explored as a nanofiller in high performance polymeric membrane for gas separation. In this regard, nanocomposite membrane of polycarbonate (PC), poly(vinylidene fluoride-*co*-hexafluoropropylene) (PVFHFP), and multiwalled carbon nanotube (MWCNT) was fabricated *via* phase inversion technique. Poly(ethylene glycol) (PEG) was employed for the compatibilization of the blend system. Two series of PC/PVFHFP/PEG were developed using purified P-MWCNT and acid functional A-MWCNT nanofiller. Scanning and transmission electron micrographs have shown fine nanotube dispersion and wetting by matrix, compared with the purified system. Tensile strength and Young's modulus of PC/PVFHFP/PEG/MWCNT-A 1–5 were found to be in the range of 63.6–72.5 MPa and 110.6–122.1 MPa, respectively. The nanocomposite revealed 51% increase in Young's modulus and 28% increase in tensile stress relative to the pristine blend. The A-MWCNT was also effective in enhancing the permselectivity $\alpha CO_2/N_2$ (31.2–39.9) of nanocomposite membrane relative to the blend membrane (21.6). The permeability P_{CO_2} of blend was 125.6 barrer; however, the functional series had enhanced P_{CO_2} values ranging from 142.8 to 186.6 barrer. Moreover, A-MWCNT loading improved the gas diffusivity of PC/PVFHFP/PEG/MWCNT-A 1–5; however, filler content did not significantly influence the CO_2 and N_2 solubility.

1. Introduction

Among carbon nanostructured materials, carbon nanotube (CNT) is one of the nanomaterials having remarkable physical and mechanical properties [1, 2]. Carbon nanotube is a hexagonal network/sheet of carbon atoms, which are rolled up into a hollow cylinder. Each end of a nanotube is capped with half of a fullerene molecule. Carbon nanotube is similar in chemical composition to graphite. Generally, two main types of nanotube are considered, that is, single-walled carbon nanotube (SWCNT) and multiwalled carbon nanotube (MWCNT). In multiwalled nanotube, there is a collection of several concentric graphene cylinders bound together by weak forces to form a Russian doll-like structure. In polymeric nanocomposite, carbon nanotube has been used as a nanofiller to form ultralight structural materials with enhanced thermal, mechanical, electrical, and optical characteristics [3–5]. Initially, nanotube production and employment in polymeric materials were not cost-effective due to expensive production procedures. However, advances in CNT synthesis have rendered improved quantity and quality of nanotube at low cost. With the mass production of carbon nanotube, advanced polymer/CNT nanocomposite with multifunctional features has gained attention in both academia and industry [6, 7]. Several potential applications of these nanocomposites have been developed such as structural materials for gas separation membrane [8–10]. Gas separation polymeric membrane is a dynamic research area due to increasing interest in carbon dioxide capture to alleviate global warming [11]. The light weight, ease of processability, and efficiency of polymeric membrane render it attractive for carbon dioxide capture relative to conventional membranes. These membranes have the ability to selectively pass one component in a gas mixture, despite rejecting others [12]. In this regard, recently, polymeric nanocomposite membranes with incorporated nanofiller have been explored. The polymeric

nanocomposite membranes have shown enhanced gas selectivity and high gas permeability compared with the neat polymeric membrane [13, 14]. Incidentally, an important class of thermoplastic polymers is polycarbonate (PC) [15]. Polycarbonate is usually considered between the commodity plastics and engineering plastics. The name polycarbonate suggests that its chemical structure consists of carbonate group. It is an easily workable, moldable, strong, and tough thermoformed material. PC also possesses fine impact and shock resistance, optical properties, and thermal resistance [16, 17]. The glass transition temperature of polycarbonate is recorded as ~ 150°C. Accordingly, polycarbonate and multiwalled carbon nanotube form an important class of nanocomposites [18–20]. The superlative mechanical and other physical properties of SWCNT and MWCNT have made them an ideal filler material for polycarbonate reinforcement. In PC/CNT nanocomposite, enhancement in Young's modulus, strength, and toughness has been considered [6, 21, 22]. In this attempt, multiwalled carbon nanotube- (MWCNT-) based nanocomposite membranes have been developed for CO_2/N_2 separation. A blend of polycarbonate (PC) and poly(vinylidene fluoride-*co*-hexafluoropropylene) (PVFHFP) was designed in this regard. Poly(ethylene glycol) (PEG) was used as compatibilizer in the blend system. The MWCNT reinforced PC/PVFHFP/PEG membranes possess fine CO_2/N_2 gas separation performance and mechanical properties relative to neat blend membrane.

2. Experimental

2.1. Materials. Polycarbonate (PC, $M_w \sim 50,000$), poly(vinylidene fluoride-*co*-hexafluoropropylene) (PVFHFP, $M_w \sim 400,000$, average $M_n \sim 130,000$), poly(ethylene glycol) (PEG, average $M_n \sim 400$), multiwalled carbon nanotube (>98% carbon basis, OD × L6–13 nm × 2.5–20 μm), and dimethylformamide (DMF, 99%) were obtained from Aldrich.

2.2. Measurement. Fourier transform infrared (FTIR) spectra were recorded in the range of 400–4000 cm^{-1} using a PerkinElmer FTIR spectrometer. Field emission scanning electron microscopy (FE-SEM) was performed using JSM5910, JEOL, Japan, to examine freeze-fractured samples. Tensile tests of all the samples were performed using Shenzhen Sans Universal Testing Machine (UTM), at ambient conditions with cross head speed of 2 mm/min and 0.5 kN load. Gas permeation tests were performed at 27°C and upstream pressure of 10 psi [23]. The value of gas permeability (P) was measured from

$$P = \frac{VL}{ART\Delta P}\frac{dP}{dt}, \tag{1}$$

where V is the downstream volume, L is membrane thickness, A is membrane area, R is the universal gas constant, T is absolute temperature, $\Delta P = p_2 - p_1$ is transmembrane pressure difference, p_2 and p_1 are upstream and downstream pressures, and dp/dt is the steady rate at which pressure increases on the downstream side.

The permselectivity (α) was calculated using

$$\alpha = \frac{P_A}{P_B}, \tag{2}$$

where P_A and P_B are permeabilities of two gases.

The diffusivity (D) was estimated from

$$D = \frac{L^2}{\theta}, \tag{3}$$

where θ is the time lag when a steady dp/dt rate is obtained on the downstream side and L is the membrane thickness.

The solubility (S) was determined from

$$S = \frac{P}{D}, \tag{4}$$

where D is diffusivity and P is permeability.

2.3. Purification and Functionalization of Multiwalled Carbon Nanotube (P-MWCNT and A-MWCNT). 1 g multiwalled carbon nanotube was refluxed in 300 mL HCl for 3 h (70°C). Then, the mixture was cooled to room temperature and poured in 300 mL of deionized water. The mixture was filtered and washed with deionized water until pH ~ 6.5. The purified nanofiller was dried at 80°C for 6 h [24]. The purified MWCNT were refluxed and sonicated at 70°C (6 h) in a mixture of 8 M sulfuric and 5 M nitric acid (3 : 1, resp.). Later, 300 mL of deionized water was added to the above mixture. The mixture was filtered using cellular membrane filter paper and washed several times with deionized water to obtain pH ~ 6.5 [25].

2.4. Polycarbonate/poly(vinylidene fluoride-co-hexafluoropropylene)/poly(ethylene glycol) (PC/PVFHFP/PEG) Membrane Formation via Phase Inversion. 0.5 g PC was dissolved in 1 mL DMF *via* 3 h sonication. Dispersion of 0.3 g PVFHFP was also prepared in 0.5 mL DMF with sonication of 2 h. The PVFHFP solution was then added to the PC solution. The mixture was refluxed for 1 h at 80°C. To the reaction flask, 0.1 g of PEG was added as compatibilizer. The mixture was again refluxed for 2 h at 80°C. The solution was cast on a glass plate using a knife. The glass plate was then immersed in aqueous solution for 0.5 h. The resulting membranes were dried at 80°C for 2 h [26].

2.5. Polycarbonate/poly(vinylidene fluoride-co-hexafluoropropylene)/poly(ethylene glycol) and Multiwalled Carbon Nanotube (PC/PVFHFP/PEG/MWCNT) Membrane Formation. The phase inversion route was also used for the formation of composite membranes. 0.5 g PC and 0.3 g PVFHFP were dissolved in DMF. 0.1 g of PEG was also added as a compatibilizer to the reaction mixture. The desired contents (1, 3, 5, and 7 wt.%) of nanofiller (P-MWCNT and A-MWCNT) were added and the mixture was refluxed for 3 h at 80°C (Figure 1). The composition of the prepared membrane samples is given in Table 1.

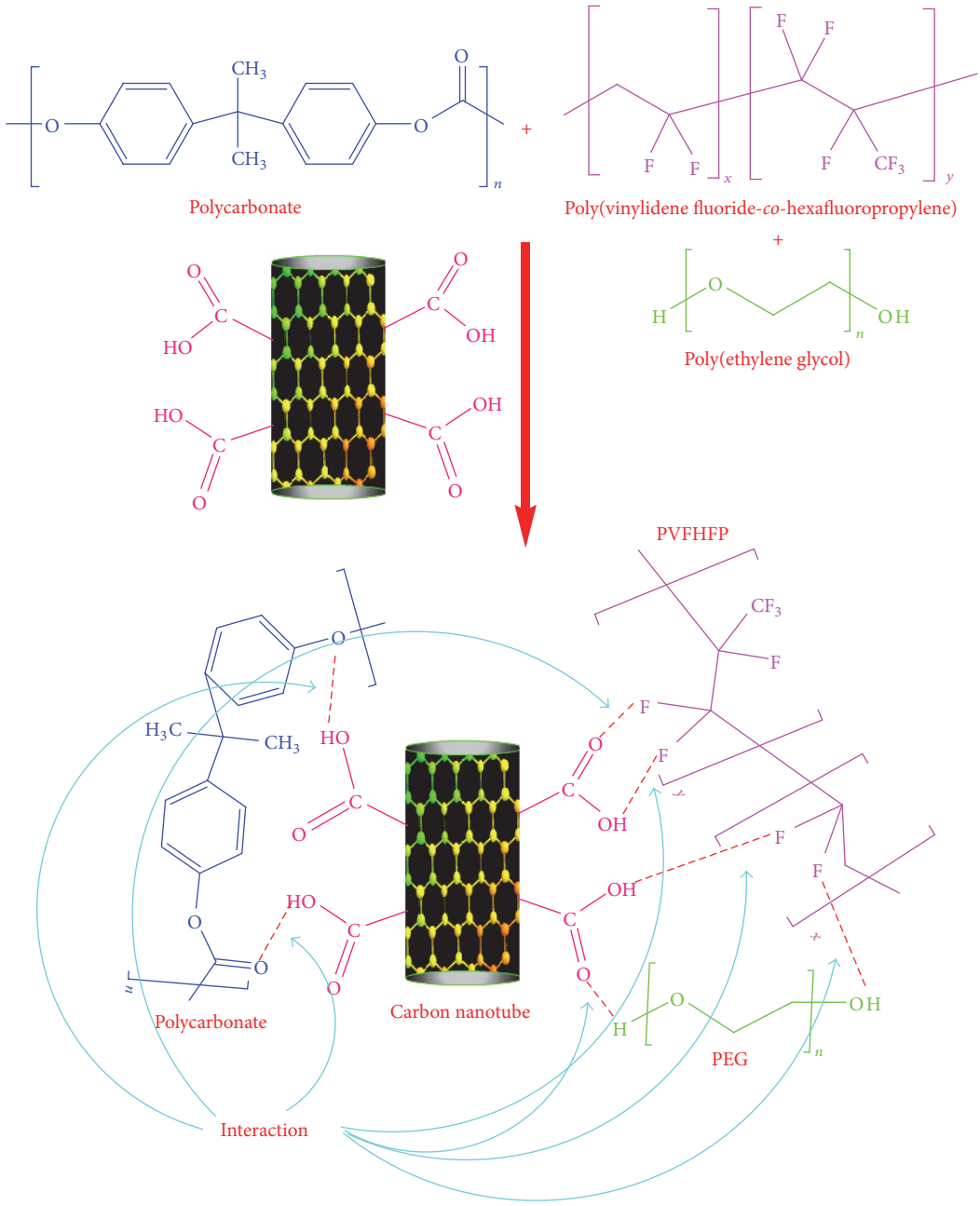

Figure 1: Formation of nanocomposite membrane.

3. Results and Discussion

3.1. Structural Analysis. FTIR spectra of purified and functional multiwalled carbon nanotube are given in Figure 2. Acid functionalization of nanotube was confirmed by the appearance of a broad peak for carboxylic acid group at 3392 cm^{-1} and carbonyl at 1609 cm^{-1}. A broad and intense peak for C–O also appeared at 1021 cm^{-1} depicting the surface modification of nanotube. FTIR spectra of PC/PVFHFP/PEG and PC/PVFHFP/PEG/A-MWCNT 1 are given in Figure 3. In the blend spectrum, characteristic peaks of aliphatic and aromatic C–H stretching vibration appeared at 2913 and 3009 cm^{-1} (Figure 3(a)). The C–O stretching vibration was found at 1244 cm^{-1}, while the carbonate C=O was located at 1670 cm^{-1} due to polycarbonate backbone. The hydroxyl group due to PEG compatibilizer appeared at 3371 cm^{-1}. The peak at 1533 cm^{-1} was due to C=C stretching vibration of the aromatic rings in matrix backbone. The C–F stretching vibration was identified as strong band at 1090 cm^{-1}. Moreover, the hydroxyl stretching vibration was observed at 3360 cm^{-1} in the case of PC/PVFHFP/PEG/A-MWCNT 1 nanocomposite membrane (Figure 3(b)). The lowering and broadening of O–H stretching vibration were due to the development of intense hydrogen bonding interaction

Table 1: Sample codes and composition used.

Sample	Composition	PC	PVFHFP	PEG	MWCNT
PC/PVFHFP/PEG blend	Polycarbonate/poly(vinylidene fluoride-*co*-hexafluoropropylene)/poly(ethylene glycol)	0.5	0.3	0.1	0
PC/PVFHFP/PEG/P-MWCNT 1	Polycarbonate/poly(vinylidene fluoride-*co*-hexafluoropropylene)/poly(ethylene glycol)/purified multiwalled carbon nanotube 1	0.5	0.3	0.1	1
PC/PVFHFP/PEG/P-MWCNT 3	Polycarbonate/poly(vinylidene fluoride-*co*-hexafluoropropylene)/poly(ethylene glycol)/purified multiwalled carbon nanotube 3	0.5	0.3	0.1	3
PC/PVFHFP/PEG/P-MWCNT 5	Polycarbonate/poly(vinylidene fluoride-*co*-hexafluoropropylene)/poly(ethylene glycol)/purified multiwalled carbon nanotube 5	0.5	0.3	0.1	5
PC/PVFHFP/PEG/P-MWCNT 7	Polycarbonate/poly(vinylidene fluoride-*co*-hexafluoropropylene)/poly(ethylene glycol)/purified multiwalled carbon nanotube 5	0.5	0.3	0.1	7
PC/PVFHFP/PEG/A-MWCNT 1	Polycarbonate/poly(vinylidene fluoride-*co*-hexafluoropropylene)/poly(ethylene glycol)/acid functional multiwalled carbon nanotube 1	0.5	0.3	0.1	1
PC/PVFHFP/PEG/A-MWCNT 3	Polycarbonate/poly(vinylidene fluoride-*co*-hexafluoropropylene)/poly(ethylene glycol)/acid functional multiwalled carbon nanotube 3	0.5	0.3	0.1	3
PC/PVFHFP/PEG/A-MWCNT 5	Polycarbonate/poly(vinylidene fluoride-*co*-hexafluoropropylene)/poly(ethylene glycol)/acid functional multiwalled carbon nanotube 5	0.5	0.3	0.1	5
PC/PVFHFP/PEG/A-MWCNT 7	Polycarbonate/poly(vinylidene fluoride-*co*-hexafluoropropylene)/poly(ethylene glycol)/acid functional multiwalled carbon nanotube 5	0.5	0.3	0.1	7

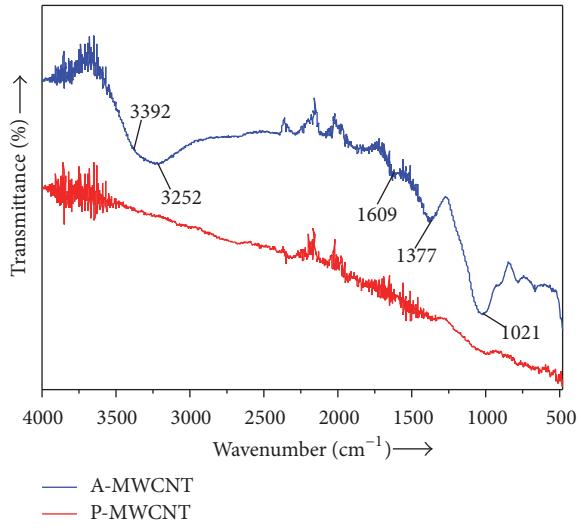

Figure 2: FTIR spectra of carbon nanotube.

between acid functional nanofiller and the blend structure. Similarly, the C=O stretching vibration was lowered to 1660 cm^{-1} owing to hydrogen bonding in matrix-nanofiller configuration. The peak at 1230 cm^{-1} indicated C–O stretching vibration. The shift of characteristic absorbance peaks of C=O carbonyl and C–O to lower wavenumber in nanocomposite membrane qualitatively indicated interaction between nanotube structure and the blend matrix. The aliphatic and aromatic C–H stretching vibrations appeared at 2890 and 3003 cm^{-1}, respectively. The peak at 1074 cm^{-1} was the characteristic of C–F functional group [27]. Here again, the lowering in frequency indicates the formation of hydrogen bonding with the electronegative fluorine functionality.

3.2. Mechanical Property Study. Table 2 reveals the tensile stress at break, Young's modulus, and elongation at break of PC/PVFHFP/PEG blend, PC/PVFHFP/PEG/P-MWCNT,

Table 2: Tensile strength, strain, and Young's modulus of PC/PVFHFP/PEG/MWCNT-based membrane.

Sample	Tensile stress at break (MPa)	Elongation at break (%)	Young's modulus (MPa)
PC/PVFHFP/PEG blend	51.9 (1.1)*	34.3 (1.1)	60.2 (1.2)
PC/PVFHFP/PEG/P-MWCNT 1	54.3 (1.2)	33.6 (1.1)	70.2 (1.1)
PC/PVFHFP/PEG/P-MWCNT 3	56.6 (1.1)	30.5 (1.2)	75.3 (1.2)
PC/PVFHFP/PEG/P-MWCNT 5	62.1 (1.3)	29.7 (1.1)	101.2 (1.3)
PC/PVFHFP/PEG/P-MWCNT 7	45.3 (1.1)	28.9 (1.2)	68.1 (1.1)
PC/PVFHFP/PEG/A-MWCNT 1	63.6 (1.2)	27.2 (1.1)	110.6 (1.1)
PC/PVFHFP/PEG/A-MWCNT 3	65.7 (1.1)	24.4 (1.1)	116.6 (1.2)
PC/PVFHFP/PEG/A-MWCNT 5	72.5 (1.2)	22.3 (1.2)	122.1 (1.1)
PC/PVFHFP/PEG/A-MWCNT 7	54.8 (1.1)	20.8 (1.1)	112.3 (1.1)

*The values in brackets show standard deviation.

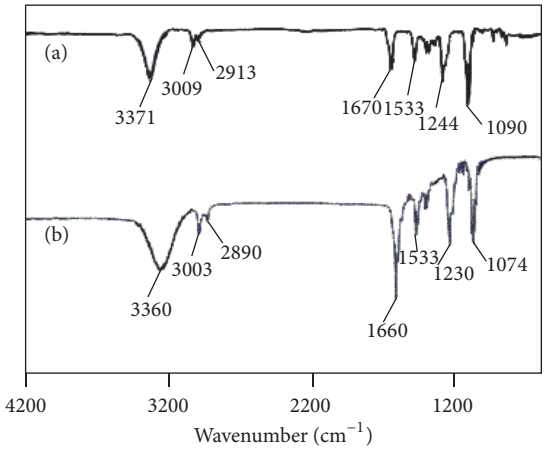

Figure 3: FTIR spectra of (a) PC/PVFHFP/PEG blend and (b) PC/PVFHFP/PEG/A-MWCNT 1 nanocomposite membrane.

and PC/PVFHFP/PEG/A-MWCNT nanocomposite membrane. In the nanocomposite membrane series, tensile strength and Young's modulus were found to increase with nanofiller loading; however, the elongation at break was found to decrease [28, 29]. Tensile strength for neat PC/PVFHFP/PEG blend membrane was found to be 51.9 MPa. The strength of PC/PVFHFP/PEG/P-MWCNT 1 membrane was observed as 54.3 MPa. The property was found to increase to 56.6 MPa with 3 wt.% nanofiller loading. Inclusion of 5 wt.% purified nanotube further improved the mechanical strength to 62.1 MPa, which was the highest value obtained for purified series. However, inclusion of 7 wt.% nanofiller decreased the tensile strength to 45.3 MPa. The effect of acid functional MWCNT addition was also studied. The tensile stress of PC/PVFHFP/PEG/A-MWCNT 1 nanocomposite was 63.6 MPa. The property was increased for PC/PVFHFP/PEG/A-MWCNT 3 (65.7 MPa). The inclusion of 5 wt.% functional filler further enhanced the tensile stress to 72.5 MPa. In this way, the tensile stress of PC/PVFHFP/PEG/A-MWCNT 5 was 28% higher than the pristine blend, while it was 14% higher than the 5 wt.% purified nanofiller sample. Here again, the addition of 7 wt.% nanofiller decreased the tensile strength to 54.8 MPa. Addition of the reinforcement up to 5 wt.% increased the mechanical properties, also reported in the literature [30]. The positive effect on tensile strength was most likely due to stiffness of nanotube layers in immobilized polymer phase and also because of nanoscale dispersion of nanofiller layer in the polymer matrix [31]. Consequently, macromolecular and carbon nanotube layer orientation contributed to the observed reinforcement effect. Nevertheless, beyond 5 wt.% nanofiller concentration, the tensile properties were found to decrease. At higher loading level, nanofillers tend to bundle together owing to intrinsic van der Waals attraction between individual nanotubes. Moreover, high aspect ratio and surface area of nanotube lead to agglomeration of nanotube in polymer matrix. Young's modulus of PC/PVFHFP/PEG/P-MWCNT 1–5 sample was increased in the range of 70.2–101.2 MPa, relative to the blend sample (60.2 MPa). The addition of functional nanofiller resulted in further improved Young's modulus in the range of 110.6–122.1 MPa for PC/PVFHFP/PEG/A-MWCNT 1–5 series. The PC/PVFHFP/PEG/A-MWCNT 5 sample revealed 51% increase in Young's modulus relative to the blend and 17% increase relative to 5 wt.% loaded purified sample. The stress-strain curves of neat blend and PC/PVFHFP/PEG/P-MWCNT and PC/PVFHFP/PEG/A-MWCNT membrane series are given in Figure 4. The tensile results showed that the functional nanotube acted as strong reinforcing agent for polycarbonate blend. Moreover, the mechanical property trend may be attributed to fine nanofiller orientation and interaction with the blend matrix, which significantly augmented the properties of resulting nanocomposite membranes. Another observation was the decreasing elongation at break of PC/PVFHFP/PEG/P-MWCNT 1–5 (33.6–29.7%) and PC/PVFHFP/PEG/A-MWCNT 1–5 series (27.2–22.3). However, the pristine PC/PVFHFP/PEG blend had higher elongation at break value of 34.3%. Consequently, the mechanical profile revealed essentially improved membrane performance and application in technical fields.

3.3. Morphology Investigation. The surface morphology of PC/PVFHFP/PEG blend and nanocomposite membranes at nanometer length scale is given in Figure 5. Assessment

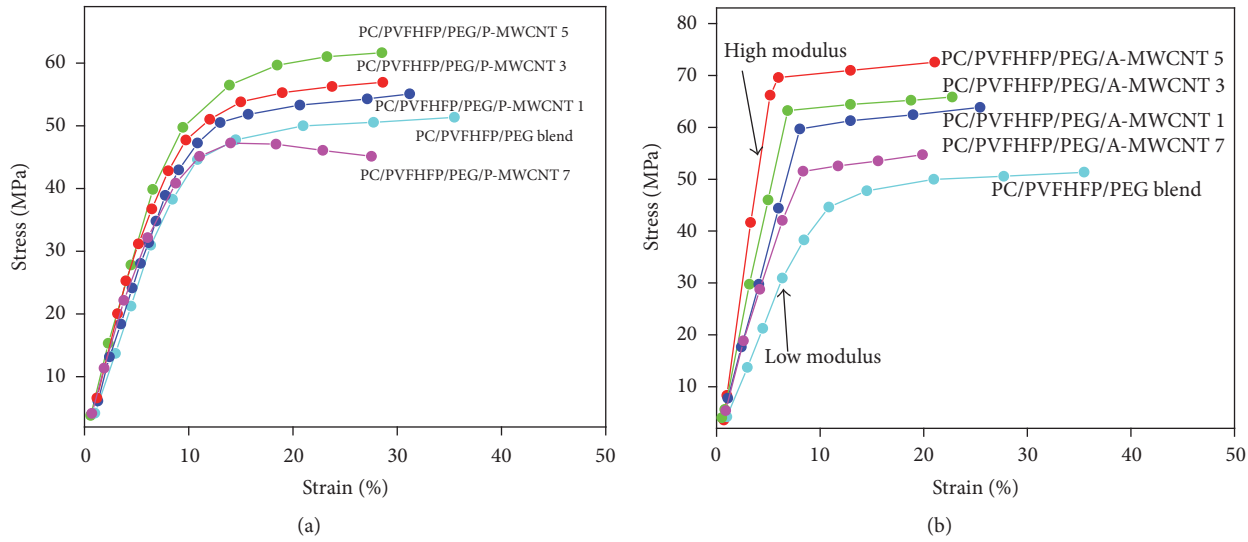

Figure 4: Stress-strain curves of (a) PC/PVFHFP/PEG/P-MWCNT and (b) PC/PVFHFP/PEG/A-MWCNT series.

of the fractured surface of pristine blend revealed two-phase morphology (Figure 5(a)). It seems that the polycarbonate formed continuous phase (the matrix), while poly(vinylidene fluoride-*co*-hexafluoropropylene) was dispersed using poly(ethylene glycol) compatibilizer. Micrographs obtained from the fracture surfaces of composite films with purified MWCNT show that the nanofiller was agglomerated in large bundles and does not disperse evenly throughout the matrix (Figures 5(b) and 5(c)). Nevertheless, the micrographs also revealed wetting of purified nanotubes by the matrix, besides their tendency to agglomerate. Figure 5(d) shows FESEM micrograph of the fracture surface of PC/PVFHFP/PEG containing 1 wt.% functionalized A-MWCNT. After functionalization, MWCNT dispersed well through the matrix and exhibited excellent wetting by polymers. The micrographs of functionalized MWCNT nanocomposite membranes with 3 and 5 wt.% nanofiller presented good dispersion as well as wetting by matrix (Figures 5(e) and 5(f)). The polymer coated functional nanotube was also observable protruding out from the fractured surface. However, the individual nanotube was not clearly visible in SEM.

3.4. Gas Separation Performance of Multiwalled Carbon Nanotube Reinforced Blend Membrane. According to the literature, gas permeability is usually influenced by nanofiller type, distribution, and matrix/nanofiller alignment [32, 33]. The permeability and permselectivity of PC/PVFHFP/PEG-based nanocomposite membrane, as a function of filler concentration, are given in Table 3. The PC/PVFHFP/PEG blend has permeability P_{CO_2} of 125.6 barrer and permselectivity $\alpha CO_2/N_2$ of 21.6. The membrane with 1 wt.% purified filler revealed permeability P_{CO_2} of 133.3 barrer and permselectivity $\alpha CO_2/N_2$ of 22.5. The CO_2 permselectivity of PC/PVFHFP/PEG-based nanocomposite membrane was increased with increasing the filler concentration. The $\alpha CO_2/N_2$ of PC/PVFHFP/PEG/P-MWCNT 3 membrane increased to 24.2, while the permeability P_{CO_2} attained the value of 134.5 barrer at 3 wt.% filler content. $\alpha CO_2/N_2$ and P_{CO_2} of PC/PVFHFP/PEG/P-MWCNT 5 were further enhanced to 27.7 and 143.3 barrer, respectively; that is, the permselectivity was 22% increased, while permeability was 12% increased with respect to the blend sample. For the functional nanotube reinforced PC/PVFHFP/PEG/MWCNT-A system, P_{CO_2} was found in the range of 142.8–186.6 barrer, while the permselectivity was in the range of 31.2–39.9. There was 32.6% increase in permeability and 45% increase in permselectivity of functional series relative to neat blend system. In this way, the properties of functional nanocomposite membrane were severalfold increased with the nanofiller addition. It seems that the acid functional nanotube was found to be more effective than the purified nanofiller in enhancing the permselectivity and decreasing the CO_2 permeability (Figure 6). Further inspection suggested that the CO_2 and N_2 diffusivity was also increased with the nanofiller loading in the membranes. Figure 7 shows that the N_2 and CO_2 diffusivity of 5 wt.% functional nanocomposite membrane was found to be higher than the blend membrane. Moreover, the nanofiller content did not significantly influence the CO_2 and N_2 solubility in the nanocomposite membranes [34]. The overall results recommended that the functional MWCNT addition up to 5 wt.% improved the gas separation properties rather than deteriorating them. In order to understand the transport mechanism through composite membrane, consideration must be given to (i) gas component being preferentially transported through the membrane; (ii) dispersed phase; and (iii) continuous phases. In membrane-based gas separation process, components are separated from their mixture by differential permeation through membranes. Inorganic fillers with molecular sieving characteristics are reinforced in polymer matrix, which allow the smaller component to pass through the membrane. Selective transport of condensable molecules with smaller size may occur through membranes *via* differential permeation

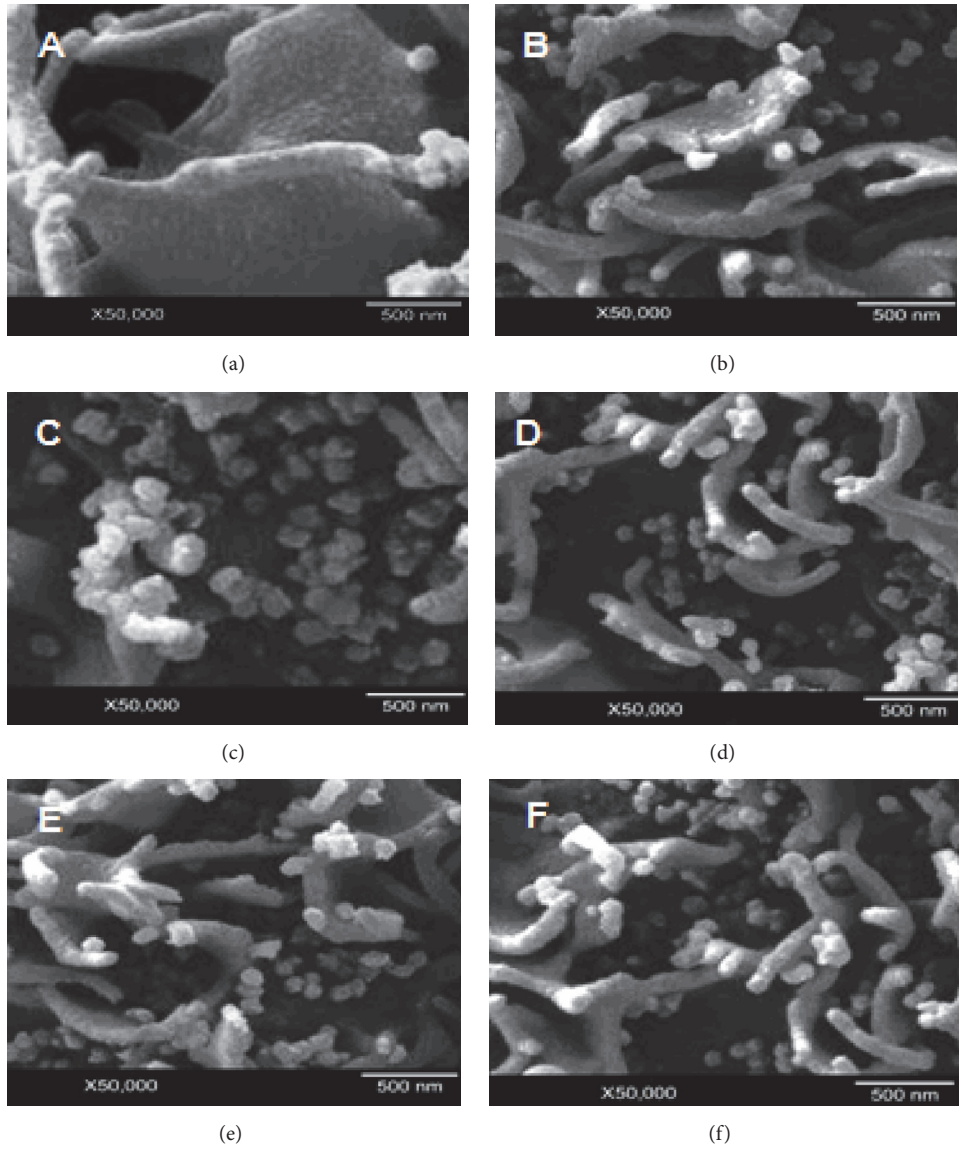

Figure 5: FESEM images of (a) PC/PVFHFP/PEG blend; (b) PC/PVFHFP/PEG/P-MWCNT 1; (c) PC/PVFHFP/PEG/P-MWCNT 5; (d) PC/PVFHFP/PEG/A-MWCNT 1; (e) PC/PVFHFP/PEG/A-MWCNT 3; and (f) PC/PVFHFP/PEG/A-MWCNT 5.

and sieving mechanism [35, 36]. In this way, the membrane enables the selective adsorption or surface diffusion of smaller and more condensable component, while excluding the less condensable component.

4. Conclusions

The functional nanotube membranes impregnated with polycarbonate/poly(vinylidene fluoride-*co*-hexafluoropropylene) and PEG compatibilizer possess fine morphology due to better compatibility and interaction of A-MWCNT with the polymer blend. Nanofiller content was varied between 1 and 5 wt.%, for a selected blend composition. The tensile strength and modulus of functional nanocomposite membranes were also enhanced relative to neat blend and purified membranes. On the other hand, the elongation at break was found to decrease. The CO_2 permeability of PC/PVFHFP/PEG/MWCNT-A nanocomposite membrane

Table 3: Gas separation performance of PC/PVFHFP/PEG/MWCNT-based membrane.

Sample	P_{CO_2} (barrer)	$\alpha CO_2/N_2$
PC/PVFHFP/PEG	125.6	21.6
PC/PVFHFP/PEG/P-MWCNT 1	133.3	22.5
PC/PVFHFP/PEG/P-MWCNT 3	134.5	24.2
PC/PVFHFP/PEG/P-MWCNT 5	143.3	27.7
PC/PVFHFP/PEG/A-MWCNT 1	142.8	31.2
PC/PVFHFP/PEG/A-MWCNT 3	149.1	32.9
PC/PVFHFP/PEG/A-MWCNT 5	186.6	39.9

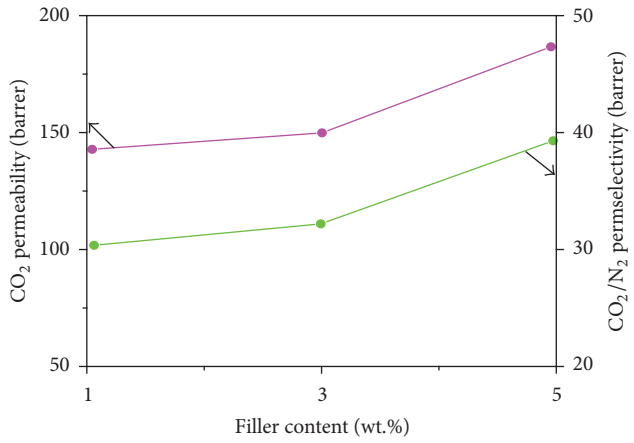

Figure 6: Permeability and permselectivity of PC/PVFHFP/PEG/A-MWCNT membranes as a function of filler content.

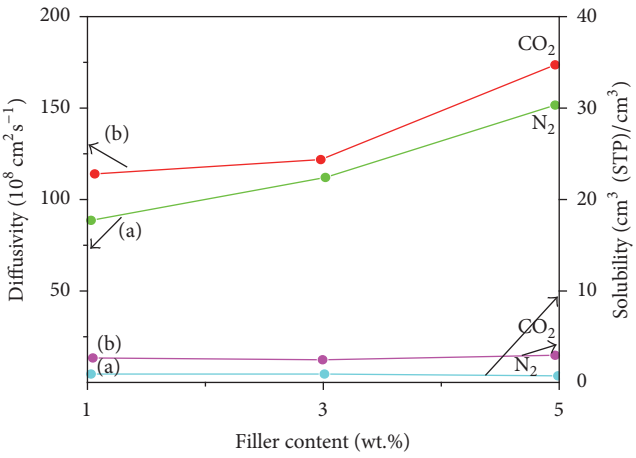

Figure 7: CO_2/N_2separation performance in terms of diffusivity and solubility for (a) PC/PVFHFP/PEG/P-MWCNT and (b) PC/PVFHFP/PEG/A-MWCNT nanocomposite membranes as a function of filler content.

was increased considerably from 142.8 to 186.6 barrer. High functional nanofiller concentration (5 wt.%) enhanced the selectivity $\alpha CO_2/N_2$ to 39.9. Moreover, the gas diffusivity of the membrane was found to be higher than that of blend membrane. Conclusively, better mechanical properties of polycarbonate blend membranes can be achieved with A-MWCNT addition without deteriorating the gas separation performance.

Competing Interests

The author declares that there are no competing interests regarding the publication of this paper.

References

[1] D. Jung, H. W. Park, G. Ma, C. Y. Lee, T. Kwon, and J.-H. Han, "Optimal synthesis of horizontally aligned single-walled carbon nanotubes and their biofunctionalization for biosensing applications," *Journal of Nanomaterials*, vol. 2016, Article ID 5140241, 8 pages, 2016.

[2] F. Navarro-Pardo, A. L. Martinez-Hernandez, and C. Velasco-Santos, "Carbon nanotube and graphene based polyamide electrospun nanocomposites: a review," *Journal of Nanomaterials*, vol. 2016, Article ID 3182761, 16 pages, 2016.

[3] A. Boonbumrung, P. Sae-oui, and C. Sirisinha, "Reinforcement of multiwalled carbon nanotube in nitrile rubber: in comparison with carbon black, conductive carbon black, and precipitated silica," *Journal of Nanomaterials*, vol. 2016, Article ID 6391572, 8 pages, 2016.

[4] S. Jabeen, A. Kausar, B. Muhammad, S. Gul, and M. Farooq, "A review on polymeric nanocomposites of nanodiamond, carbon nanotube, and nanobifiller: structure, preparation and properties," *Polymer-Plastics Technology and Engineering*, vol. 54, no. 13, pp. 1379–1409, 2015.

[5] Z. Akram, A. Kausar, and M. Siddiq, "Review on polymer/carbon nanotube composite focusing polystyrene microsphere and polystyrene microsphere/modified CNT composite: preparation, properties, and significance," *Polymer-Plastics Technology and Engineering*, vol. 55, no. 6, pp. 582–603, 2015.

[6] Z. Spitalsky, D. Tasis, K. Papagelis, and C. Galiotis, "Carbon nanotube-polymer composites: chemistry, processing, mechanical and electrical properties," *Progress in Polymer Science*, vol. 35, no. 3, pp. 357–401, 2010.

[7] T. A. Saleh and V. K. Gupta, "Processing methods, characteristics and adsorption behavior of tire derived carbons: a review," *Advances in Colloid and Interface Science*, vol. 211, pp. 93–101, 2014.

[8] S. M. Sanip, A. F. Ismail, P. S. Goh, T. Soga, M. Tanemura, and H. Yasuhiko, "Gas separation properties of functionalized carbon nanotubes mixed matrix membranes," *Separation and Purification Technology*, vol. 78, no. 2, pp. 208–213, 2011.

[9] P. S. Goh, A. F. Ismail, S. M. Sanip, B. C. Ng, and M. Aziz, "Recent advances of inorganic fillers in mixed matrix membrane for gas separation," *Separation and Purification Technology*, vol. 81, no. 3, pp. 243–264, 2011.

[10] S. T. Muntha, A. Kausar, and M. Siddiq, "Progress in applications of polymer-based membranes in gas separation technology," *Polymer-Plastics Technology and Engineering*, vol. 55, no. 12, pp. 1282–1298, 2016.

[11] O. Breuer and U. Sundararaj, "Big returns from small fibers: a review of polymer/carbon nanotube composites," *Polymer Composites*, vol. 25, no. 6, pp. 630–645, 2004.

[12] A. Brunetti, F. Scura, G. Barbieri, and E. Drioli, "Membrane technologies for CO_2 separation," *Journal of Membrane Science*, vol. 359, no. 1-2, pp. 115–125, 2010.

[13] A. L. Ahmad, Z. A. Jawad, S. C. Low, and S. H. S. Zein, "A cellulose acetate/multi-walled carbon nanotube mixed matrix membrane for CO_2/N_2 separation," *Journal of Membrane Science*, vol. 451, pp. 55–66, 2014.

[14] R. Khalilpour, K. Mumford, H. Zhai, A. Abbas, G. Stevens, and E. S. Rubin, "Membrane-based carbon capture from flue gas: a review," *Journal of Cleaner Production*, vol. 103, pp. 286–300, 2015.

[15] Y. Liu, X. Zhu, S. Wang, and M. Zhao, "Surface imprinted superparamagnetic nanoparticles for rapid and efficient extraction of bisphenol A from water samples," *Journal of the Chinese Advanced Materials Society*, vol. 1, no. 2, pp. 166–176, 2013.

[16] R. Patel, S. J. Kim, D. K. Roh, and J. H. Kim, "Synthesis of amphiphilic PCZ-r-PEG nanostructural copolymers and their

use in CO_2/N_2 separation membranes," *Chemical Engineering Journal*, vol. 254, pp. 46–53, 2014.

[17] A. F. Bushell, M. P. Attfield, C. R. Mason et al., "Gas permeation parameters of mixed matrix membranes based on the polymer of intrinsic microporosity PIM-1 and the zeolitic imidazolate framework ZIF-8," *Journal of Membrane Science*, vol. 427, pp. 48–62, 2013.

[18] W. Zhang, J. Suhr, and N. Koratkar, "Carbon nanotube/polycarbonate composites as multifunctional strain sensors," *Journal of Nanoscience and Nanotechnology*, vol. 6, no. 4, pp. 960–964, 2006.

[19] P. Pötschke, M. Abdel-Goad, I. Alig, S. Dudkin, and D. Lellinger, "Rheological and dielectrical characterization of melt mixed polycarbonate-multiwalled carbon nanotube composites," *Polymer*, vol. 45, no. 26, pp. 8863–8870, 2004.

[20] M. Abdel-Goad and P. Pötschke, "Rheological characterization of melt processed polycarbonate-multiwalled carbon nanotube composites," *Journal of Non-Newtonian Fluid Mechanics*, vol. 128, no. 1, pp. 2–6, 2005.

[21] J. N. Coleman, U. Khan, W. J. Blau, and Y. K. Gun'ko, "Small but strong: a review of the mechanical properties of carbon nanotube-polymer composites," *Carbon*, vol. 44, no. 9, pp. 1624–1652, 2006.

[22] K. H. Kim and W. H. Jo, "A strategy for enhancement of mechanical and electrical properties of polycarbonate/multi-walled carbon nanotube composites," *Carbon*, vol. 47, no. 4, pp. 1126–1134, 2009.

[23] M. Ulbricht, "Advanced functional polymer membranes," *Polymer*, vol. 47, no. 7, pp. 2217–2262, 2006.

[24] A. Kausar, A. Hussain, M. Y. Khan, and M. Siddiq, "Fuel cell membranes prepared from multi-walled carbon nanotubes and silica nanotubes-filled sulfonated polyamide/sulfonated polystyrene porous blend films," *Journal of Plastic Film and Sheeting*, vol. 30, no. 3, pp. 314–336, 2014.

[25] N. Mehwish, A. Kausar, and M. Siddiq, "Polyvinylidene-fluoride/poly(styrene-butadiene-styrene)/silver nanoparticle-grafted-acid chloride functional MWCNTs-based nanocomposites: preparation and properties," *Polymer-Plastics Technology and Engineering*, vol. 54, no. 5, pp. 474–483, 2015.

[26] I. Pinnau and W. J. Koros, "Structures and gas separation properties of asymmetric polysulfone membranes made by dry, wet, and dry/wet phase inversion," *Journal of Applied Polymer Science*, vol. 43, no. 8, pp. 1491–1502, 1991.

[27] A. I. Gopalan, P. Santhosh, K. M. Manesh et al., "Development of electrospun PVdF-PAN membrane-based polymer electrolytes for lithium batteries," *Journal of Membrane Science*, vol. 325, no. 2, pp. 683–690, 2008.

[28] J. O'Brien-Abraham, M. Kanezashi, and Y. S. Lin, "A comparative study on permeation and mechanical properties of random and oriented MFI-type zeolite membranes," *Microporous and Mesoporous Materials*, vol. 105, no. 1-2, pp. 140–148, 2007.

[29] M.-D. Jia, K.-V. Pleinemann, and R.-D. Behling, "Preparation and characterization of thin-film zeolite-PDMS composite membranes," *Journal of Membrane Science*, vol. 73, no. 2-3, pp. 119–128, 1992.

[30] A. Kausar and S. T. Hussain, "Effect of multi-walled carbon nanotube reinforcement on the physical properties of poly(thiourea-azo-ether)-based nanocomposites," *Journal of Plastic Film and Sheeting*, vol. 29, no. 4, pp. 365–383, 2013.

[31] X. Zhang, T. Liu, T. V. Sreekumar et al., "Poly(vinyl alcohol)/SWNT composite film," *Nano Letters*, vol. 3, no. 9, pp. 1285–1288, 2003.

[32] D. Q. Vu, W. J. Koros, and S. J. Miller, "Mixed matrix membranes using carbon molecular sieves: I. Preparation and experimental results," *Journal of Membrane Science*, vol. 211, no. 2, pp. 311–334, 2003.

[33] T. C. Merkel, B. D. Freeman, R. J. Spontak et al., "Sorption, transport, and structural evidence for enhanced free volume in poly(4-methyl-2-pentyne)/fumed silica nanocomposite membranes," *Chemistry of Materials*, vol. 15, no. 1, pp. 109–123, 2003.

[34] J. Ahn, W.-J. Chung, I. Pinnau, and M. D. Guiver, "Polysulfone/silica nanoparticle mixed-matrix membranes for gas separation," *Journal of Membrane Science*, vol. 314, no. 1-2, pp. 123–133, 2008.

[35] S. Sircar, M. B. Rao, and C. M. A. Thaeron, "Selective surface flow membrane for gas separation," *Separation Science and Technology*, vol. 34, no. 10, pp. 2081–2093, 1999.

[36] T. T. Moore, R. Mahajan, D. Q. Vu, and W. J. Koros, "Hybrid membrane materials comprising organic polymers with rigid dispersed phases," *AIChE Journal*, vol. 50, no. 2, pp. 311–321, 2004.


Journal of
Nanotechnology

International Journal of
Corrosion

International Journal of
Polymer Science

Smart Materials
Research

Journal of
Composites

BioMed
Research International
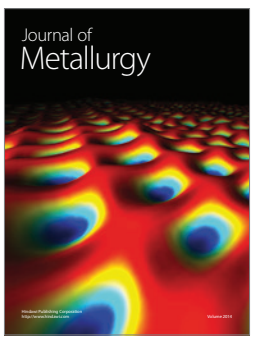
Journal of
Metallurgy

Journal of
Materials

Hindawi
Submit your manuscripts at
http://www.hindawi.com
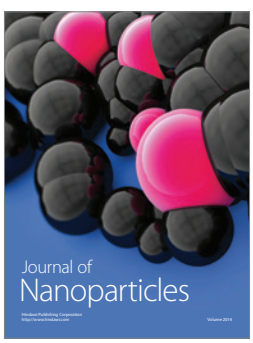
Journal of
Nanoparticles
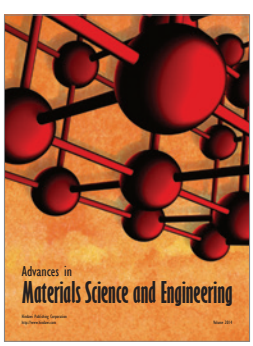
Advances in
Materials Science and Engineering
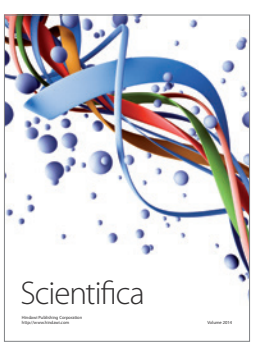
Scientifica
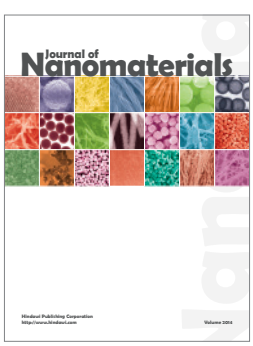
Journal of
Nanomaterials

The Scientific
World Journal

International Journal of
Biomaterials
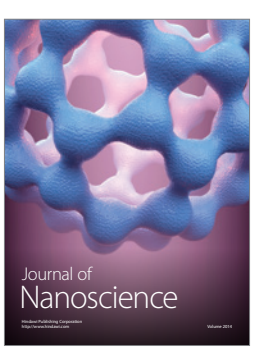
Journal of
Nanoscience

Journal of
Coatings
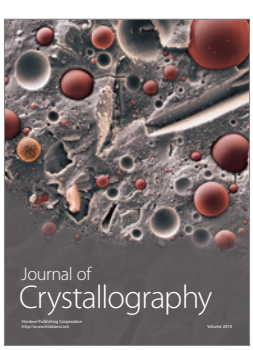
Journal of
Crystallography

Journal of
Ceramics
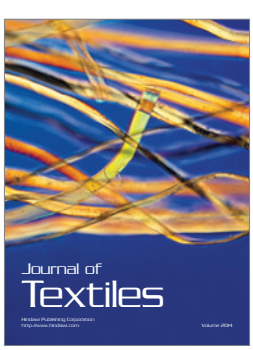
Journal of
Textiles